SPANDIDOS PUBLICATIONS

ONCOLOGY LETTERS 16: 4607-4613, 2018

Texture features and pharmacokinetic parameters in differentiating benign and malignant breast lesions by dynamic contrast enhanced magnetic resonance imaging

QINGLIANG NIU[1], XIAOMEI JIANG[1], QIN LI[1], ZHAOLONG ZHENG[1], HANWANG DU[1], SHASHA WU[1] and XUEXI ZHANG[2]

[1]Department of Radiology, WeiFang Traditional Chinese Hospital, Wei Fang, Shandong 255036; [2]GE Healthcare, Shanghai 200000, P.R. China

Received December 7, 2017; Accepted May 15, 2018

DOI: 10.3892/ol.2018.9196

Abstract. Dynamic contrast enhanced magnetic resonance imaging (DCE-MRI) has become a powerful tool for the diagnosis of breast cancer in the clinical setting due to its high sensitivity and specificity. Pharmacokinetic parameters, including Ktrans and area under the curve (AUC), and texture features derived from DCE-MRI have been used to specify the characteristics inside tumors. In the present study, 56 patients (average age 45.3±11.1; range 25-69 years) with histopathologically proved breast tumors were analyzed using the pharmacokinetic parameters and texture features. Malignant tumors displayed higher Ktrans and AUC values than the benign, Ktrans exhibited a significantly difference between the malignant and benign tumors (P=0.001) compared with the AUC values (P=0.029); texture features from DCE-MRI images and pharmacokinetic parameter maps also showed a good diagnostic ability. Alongside the routine method, principal components analysis (PCA) and Fisher discriminant analysis (FDA) were employed on these texture features to differentiate the breast lesions automatically. The Factor-1 scores of PCA were used to divide the patients into two groups, and the diagnosing accuracies of the FDA method on the texture features from DCE-MRI images, Ktrans maps, AUC maps were 93, 98 and 98%, with a cross validation accuracies of 82, 77 and 77%, respectively. To conclude, pharmacokinetic parameters, texture features and the combined computer-assisted classification method were discussed. All method involved in this study may be a potential assisted tool for radiological analysis on breast.

Correspondence to: Dr QingLiang Niu, Department of Radiology, WeiFang Traditional Chinese Hospital, 666 Weizho Road, Wei Fang, Shandong 255036, P.R. China
E-mail: qingliangniu@126.com

Key words: dynamic contrast enhanced magnetic resonance imaging, pharmacokinetic parameters, texture analysis, principal component analysis, Fisher discriminant analysis

Introduction

Breast cancer is a common malignant disease in women. Besides mammography and echography, MR imaging is of great significant in breast cancer diagnosis since its higher sensitivity and specificity (1). Depends on the abundant imaging sequences, MR imaging provides a wealth of morphological information for the diagnosis of breast disease. Multiple MR sequences describe the breast tumors in different aspects, dynamic contrast enhanced magnetic resonance imaging (DCE-MRI) requires interpretation of four-dimensional DCE data and relies on reader expertise, which could lead to a substantial amount of false positive results.

GBCA is a commonly used intravenous contrast agent for DCE-MRI, which induces an increment in the longitudinal relaxation rate, exhibited as an enhancement in the signal intensity of T1-weighted images. The pharmacokinetic parameters (Ktrans, etc.) could be obtained by fitting an appropriate model to the signal intensity time course of serial acquisition T1-weighted images after an injected GBCA into a tissue of interest (2). Several researches have proven that these parameters changes corresponded to the damage of microstructure in tumor tissues (3-5).

Texture feature is a quite abstract concept for medical imaging, it is an important surface characteristic used to identify and recognize objects, for which it might qualified the ability to describe the internal structures of lesion tissues (6). Texture extracted from breast DCE images enabled rich properties of region of interest (ROI) areas which were also useful for diagnosing different types breast lesions (7).

Texture feature represents the appearance of the medical images and considers how its pixel intensity were distributed (8), it also focuses on the intensity distribution and the relationships of neighboring pixels. Various texture analysis approaches tend to represent the examined textures from different perspectives. Texture analysis was also sensitivity to the subtle changes of the tissues that might ambiguously for human. It has been successfully used in several radiological studies, including subchondral bone, glioma tumor, distinction analysis of invasive adenocarcinoma and pre-invasive or minimally invasive adenocarcinoma (9-11).

Previously researches prefer to explore the variances of texture parameters between different types of diseased tissue. Loose *et al* (12) evaluated the Haralick textures on DCE-MRI data for the differentiation of Breast Tumor Lesions, Toshiaki *et al* (13) adopted the histogram analysis to the evaluation of vascular permeability in glioma. On the other hand, chemometric methods such as principal components analysis (PCA), support vector machine (SVM), linear discriminant analysis (LDA), have been employed to the discriminant analysis of different types of lesions (9,14,15), which aims to access the overall changes in multi-texture parameters.

In the present study, pharmacokinetic parameters, as well as the texture parameters that obtained from the DCE-MR imaging and parameter maps were discussed, PCA and Fisher discriminant analysis (FDA) were adopted to differentiate the benign and malignant breast tumors based on the textures, respectively. As to our best knowledge, this is the first try to evaluate the diagnostic efficiency of FDA method on breast tumors.

Materials and methods

Patients data. The present study was approved by the institutional review board of The Wei Fang Traditional Chinese Hospital. From December 2016 to June 2017, 56 patients with an average age of 45.3±11.1 years (25-69 years) were retrospectively enrolled. Informed consent was signed before the patients underwent contrast enhanced MR examination. Pathological examinations were performed to confirm the MR examination results. All patients were sequenced from 1 to 56 according to examination date. Fifty-six patients (23 cancer tumors, 33 benign tumors) were divided into malignant and benign group, and the benign case including breast adenoma and intraductal papilloma.

The patient selection criteria of the present study were as follows: i) All lesions were histopathological confirmed by breast surgery; ii) MR dynamic enhancement was performed no >30 days before surgery or biopsy.

MRI protocol. An MRI scan of the whole breast was performed using a 3T whole-body scanner (GE Discovery MR 750; GE Healthcare, Milwaukee, WI, USA) equipped with a dedicated 8-channel double-breast phased-array coil in prone position. Breathe training was given before MRI scan.

A series of unenhanced MRI scanning sequence were performed first, multi-flip angle (5, 10 and 15˚C) T1 Mapping was collected firstly with only one phase, respectively. DCE MR imaging was collected using vibrant sequence with the following parameters: Repetition time/echo time=4.1/2.1 ms, flip angle=10˚C, slice thickness=4 mm, matrix size=256x256 pixels, number of slices=120, and the field of view (FOV) was adjusted according to the breast volume. For each patient, a total of 30 acquisitions were obtained.

Thirty measurements with a temporal spacing of ~10 sec. At the beginning of DCE-MRI, a baseline acquisition was collected with two unenhanced phase scans, a bolus of 0.1 mmol/kg gadolinium contrast agent (Omniscan; GE Healthcare, Shanghai, China) was injected intravenously at a rate of 4 ml/sec followed by 20 ml saline flush through antecubital vein at the third acquisition. The scan duration after bolus injection was ~380 sec.

Pharmacokinetic parameters and texture features. The DCE-MRI data were transferred into Omni-Kinetic software (GE Healthcare) to obtain the perfusion and permeability parameters of the lesion areas in breast, using the dual-compartment pharmacokinetic model of Extended Tofts Linear (16,17). This model evaluates Ktrans, V_e, V_p and K_{ep} values by analog the EES space in tissues. Arterial input function (AIF) describes the time-dependent contrast agent input to the ROI (18), Subsequently, the semi-quantitative parameters, such as the slope, maximum enhancement, and area under the curve (AUC) were computed based on the model in software.

ROIs were selected based on enhanced T1-weighted images and then responded to the pharmacokinetic maps. For each breast lesions, 1-3 ROI with 10-30 mm^2 size were manually positioned on the T1WI imaging by an experienced radiologist (Fig. 1). In Fig. 1, a benign and a malignant lesion was clearly exhibited (Fig. 1A and B), a circle or a polygon ROI would be drawn manually according to the shapes of lesion.

The heterogeneity analysis (i.e. histogram, Gray-level co-occurrence matrix, etc.) was automatically calculated by the Omni-Kinetic software. For each patient, all the texture features were obtained from DCE-MRI images, Ktrans and AUC maps, respectively. Texture features from DCE-MRI images were generated only using arterial phase images according to the AIF curves. All ROIs used to the texture analysis were corresponded to the pharmacokinetic calculation parts.

Different computing methods depicted the ROI pixel distribution from different aspects. Histogram described the pixel distribution, while the Gray-level co-occurrence matrix explained the relationship of adjacent pixels (19). In this study, totally 67 texture features from 4 different calculation methods, were achieved as below: First Order (n=14), Histogram (n=15), Grey level co-occurrence matrix (GLCM, n=13), Haralick matrix (n=9), and grey level run length matrix (GLRLM, n=16).

Statistical analysis. PCA and FDA was carried out in IBM SPSS Statistics software (version 19.0; BM SPSS, Chicago, IL, USA) which is a multivariate data analysis software. PCA method extracted the principal component information of the texture dataset, the first principal component scores could reflect the type of each samples in the patient dataset grossly. FDA is a classical analytical technique for feature extraction and classification, a mapping was first calculated to reduce the dimension of texture dataset, then a linear discriminant analysis was built based on the variance analysis so that several groups or classes could be discriminated as clearly as possible (20-22). One-way analysis of variance (ANOVA) test was performed for the Ktrans and AUC values using the software of Origin 8.0 (OriginLab, Northampton, MA, USA) (23).

Results

DCE-MR images of two patients with breast lesions were shown in Fig. 2, the corresponding pharmacokinetic parameter maps that calculated by the Extended Tofts Linear model

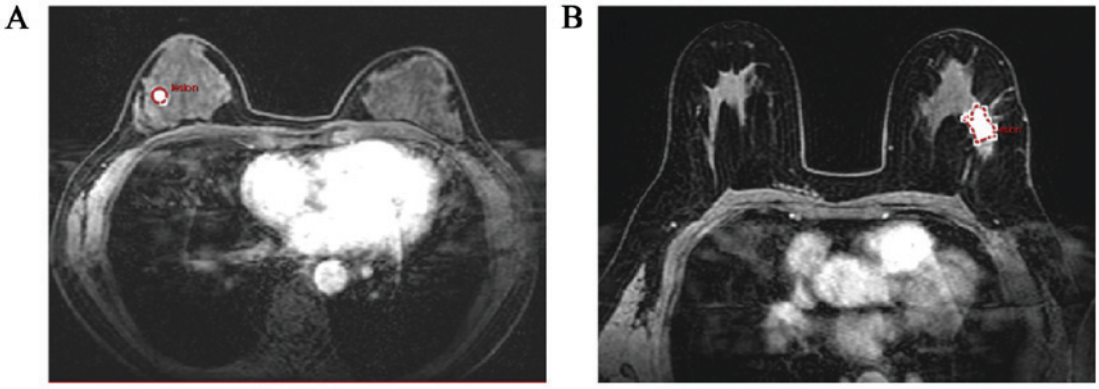

Figure 1. ROI selection on the T1WI images of patients, a round or polygonal ROI was obtained as shown in (A) and (B). ROI, region of interest

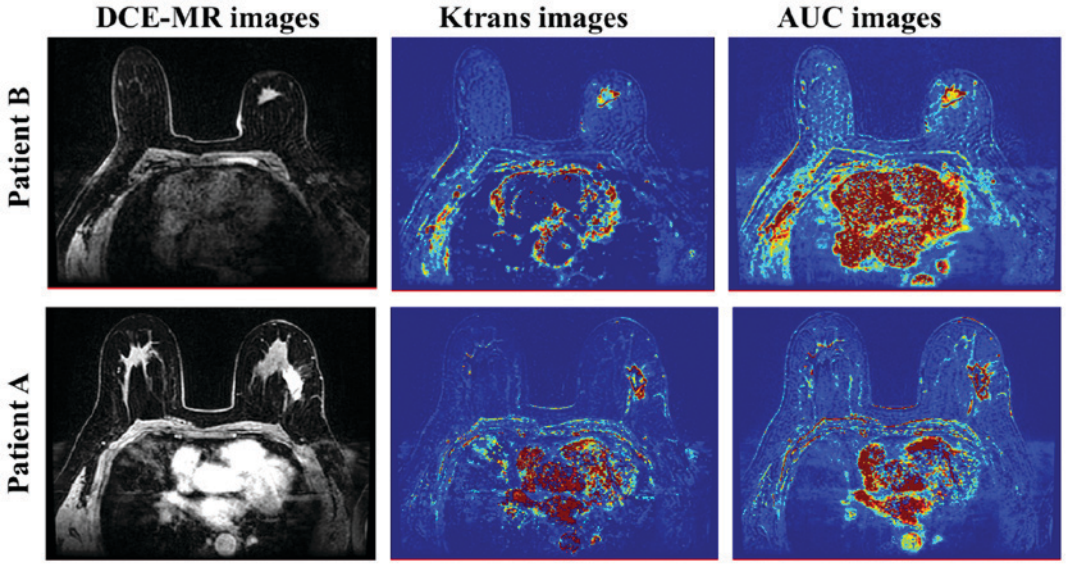

Figure 2. Ktrans and AUC images derived from the DCE-MRI images by Extended Tofts Linear model. The lesion areas were obviously spotlighted in the parameter maps. AUC, area under the curve; DCE-MRI, dynamic contrast enhanced magnetic resonance imaging.

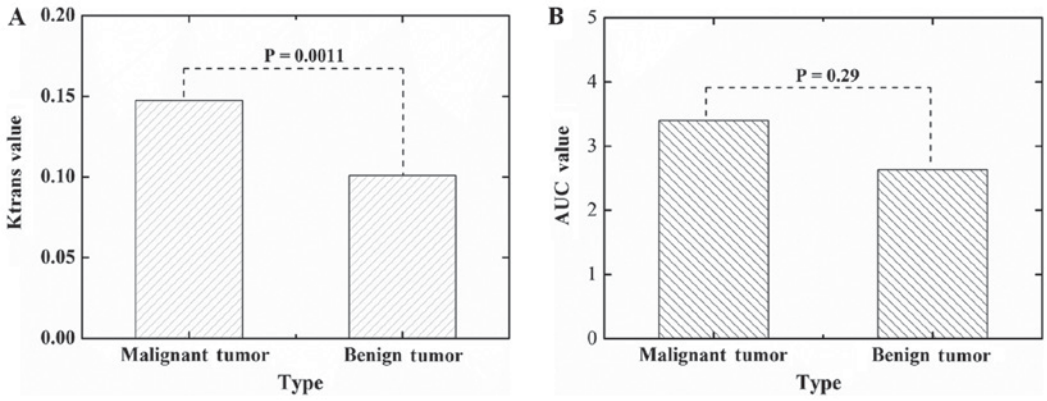

Figure 3. One-way analysis of variance tests on the (A) Ktrans and (B) AUC values for malignant and benign breast tumors. AUC, area under the curve.

were also gave out, including Ktrans images and AUC images. The lesion regions were obviously highlighted in the parameter images, which indicated a more higher permeability and perfusion when compared to the adjacent tissues (24,25).

One-way analysis of variance (ANOVA) test was performed for the Ktrans and AUC values using the software of Origin 8.0. In this study, a significant difference on the Ktrans values was found between the malignant breast tumors and benign breast tumors (P=0.0011, Fig. 3A). However, the ANOVA test on the AUC values showed no significant differences (P=0.29), we could not characterize the benign and malignant tumors only according the averaged AUC values of the two groups samples.

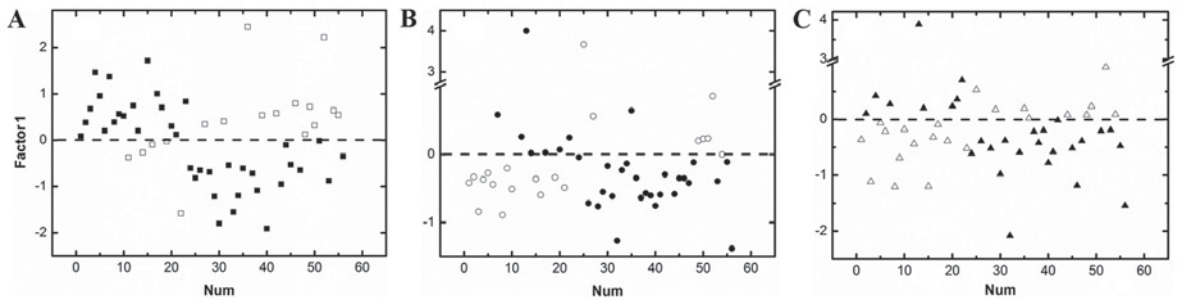

Figure 4. The first component scores of PCA on the texture parameters from DCE-MR images (A), Ktrans images (B) and AUC images (C). PCA, principal components analysis.

Table I. ANOVA tests on the texture features from T1WI image, AUC and Ktrans maps.

Method	Texture feature	T1WI image	Ktrans maps	AUC map
Haralick matrix	Difference entropy	P<0.05	P<0.05	P<0.05
	Inverse difference moment	P<0.05	P<0.05	P<0.05
Grey level run-length matrix	Min intensity	P>0.05	P<0.05	P<0.05
	Max intensity	P>0.05	P>0.05	P>0.05
	Max size	P>0.05	P<0.05	P>0.05
	Long run low grey level emphasis	P<0.05	P<0.05	P<0.05
	Long run high grey level emphasis	P>0.05	P>0.05	P>0.05

ANOVA, one-way analysis of variance; AUC area under the curve.

Table II. FDA method on DCE-MRI images, Ktrans and AUC maps.

		Predicted			
Imaging	Type	Malignant	Benign	Discriminant accuracy (%)	Discriminant accuracy (%)
DCE-MR images	Malignant	21	2	91	93
	Benign	2	31	94	
Ktrans maps	Malignant	23	0	100	98
	Benign	1	32	97	
AUC maps	Malignant	23	0	100	98
	Benign	1	32	97	

FDA, Fisher discriminant analysis; DCE-MRI, dynamic contrast enhanced magnetic resonance imaging; AUC area under the curve.

Previously studies have revealed the potential diagnostic ability of texture feature from medical images. In this study, 67 texture features were extracted from the DCE-MRI images and the pharmacokinetic parameter maps, including Ktrans and AUC (as shown in Fig. 1), respectively.

PCA was firstly applied to the texture features of the DCE-MRI images, Ktrans and AUC maps, respectively, without any pre-processing. Recently study has tried to use the PCA method followed by adjusted model to analysis breast DCE-MRI images, and an objective diagnostic tool was established (26). However, PCA could also be used as an early attempt to classify unknown datasets, as shown in Fig. 4, the Factor-1 score values of PCA could roughly divide the 56 patients into two groups, the hollow squares (□), circles (○), and triangles (Δ) were the misjudged cases (Fig. 4).

To achieved the better discriminant accurate results of texture features, further research was required. Spearman correlation analysis was firstly performed to reduce the redundancy of the texture feature on T1WI images, Ktrans and AUC maps. One texture feature would be discard once the Spearman correlation coefficient between two texture features was >0.9, the correlation analysis was carried out for all texture features.

Totally seven common features were left in the three texture feature datasets (Table I). One-way ANOVA tests were

calculated for the seven common features on T1WI, Ktrans and AUC maps, respectively. Haralick matrix showed a promising differentiation ability for the malignant and benign tumors, both on the T1WI images and pharmacokinetic parameter maps ($P<0.05$), on the other hand, the Long-Run-Low Grey-Level-Emphasis of GLRLM exhibit the same ability (6,8).

FDA method was also built based on the three texture features datasets that have underwent the spearman correlation analysis, the discriminant accuracies of FDA method on the DCE-MRI images, Ktrans maps and AUC maps were 93, 98 and 98%, respectively (Table II). Cross validation analysis was performed on the FDA method for DCE-MRI images, Ktrans and AUC maps with the discriminant accuracies of 82, 77 and 77%, respectively. The promising results of FDA and cross validation result indicated that FDA method could be a reliable tool to diagnose the breast lesions.

Discussion

In this study, a comprehensive exploring, including pharmacokinetic parameters, texture features, and the created FDA method, was adopted to quantitatively evaluate the malignant and benign breast tumors. All these three aspects showed a promising result for the breast patients. This experiment provided a preoperative clinical assessment of breast tumor.

In recent years, pharmacokinetic parameters have been adopted to explore the penetration and perfusion changes inside the tumors (27-29). In the present study, the semi-quantitative parameters (e.g. AUC) and quantitative parameters (e.g. Ktrans) were calculated, Ktrans values showed a better diagnostic ability between the malignant and benign breast tumors than AUC. This difference of Ktrans and AUC values has indicated the increment of microvascular permeability in the malignant tumors. Ktrans is a well-established permeability parameter of tumors, which was obtained with DCE-MRI and has been applied to many kinds of tumors. It reflects the diffusive transport of contrast agent across the capillary endothelium (16,17). In this particular circumstance, Ktrans might directly reveal the microstructure changes inside tumors than AUC values. AUC described the areas under the arterial input function (AIF) that obtained by the Omni-Kinetic software. No significance differences were found between the benign and malignant breast tumors. The AIF curves were slightly different among the patients, which were easily affected by the machine and scanning mode. The AUC values might be unsteadily. The results in this study indicated that more attentions should be gave to the Ktrans values rather than AUC, pharmacokinetic parameters depict tumors based on the relationships between the permeability changes and biological characteristics, which might be have a better expression on the tumors.

Compared to pharmacokinetic parameters, texture features are a quite abstract concept for medical images. It considers the pixel distribution in ROIs through engineering methods. Although lots of researches have refer to these areas, some basic concepts were still ambiguous; texture parameters exhibit excellent skills on the tumors assessment and grade, survival prediction for cancer patients, evaluation of tumor therapy and prediction distant metastasis (30-32). However, how to define the texture features in medical images were still questions that need to be explained urgently. In this study, texture features on DCE-MRI images, Ktrans and AUC maps gave out difference results, For the seven common texture features that underwent spearman correlation analysis, five texture features from Ktrans map exhibit significant difference. On the other hand, difference entropy, inverse difference moment of Haralick matrix and the long-run-low grey-level-emphasis of GLRLM showed a promising ability on the three types of images. All the significant texture features characteristic the breast tumors in different aspects. The research is ongoing in our department to reveal its clinical sense or to connect the texture feature to any related clinical standards.

In addition to explore the diagnostic value of every single texture feature, regression analysis was the common way to find out the capacity of whole texture features (33,34). FDA was adopted in this study, which was easily built without strictly application restrictions. The discriminant accuracies of FDA on the DCE-MRI images, Ktrans and AUC maps were 93, 98 and 98%. A promising cross validation result on the DCE-MRI images, Ktrans and AUC maps were also achieved. The results indicated the feasibility of FDA method on breast tumors. However, some limitations should be acknowledged in this mathematical regression analysis. Firstly, Since the limitation of patient size, further investigation with much larger patient sample sizes should be included to improve the differentiation accuracies and model stability. Secondly, in this study, the patients were only divided into benign and malignant groups, more patients should be involved to specify the disease of benign and malignant breast tumors, an overall analysis on the breast tumors would be cleared once enough patients were given. Thirdly, texture analysis and the regression were generated using arterial phase images, some slight differences might be existed between different phase images, which was not discussed in this study.

The volume data of all breast tumors were obtained on the AW workstation of GE Discovery MR 750, Specified morphological data in tumors, such as surface area, were also derived from the Omini-kinetic software. Since the limitation of the patient amount, tumor morphological description was not regarded as an influential factor in this study. It would be essential and interesting to clarify the pharmacokinetic parameter changes of tumors with different size. On the other hand, metastatic lymph node plays as a significant role for tumors, the prediction of lymph node metastasis has begun to be involved in other fields with excellent results (35). Thus, the investigation of metastatic lymph node in breast cancer could also be feasible by the methods adopted in the research. Related researches were ongoing in our department.

Compared to the previous study that either focused on the analysis of each texture feature or emphasis the importance and potential of regression model, this study explored the pharmacokinetic parameters, texture features and the regression model on breast tumors, a comprehensive analysis were carried out in this study to improve understanding of quantitative parameters on breast tumors.

In conclusion, pharmacokinetic parameters and texture features provide quantitative measures of heterogeneity in breast tumors at different aspect. In this study, all parameters showed a valuable ability in breast lesion discrimination and characterization. On the other hand, the combination of

regression model with quantitative parameter also exhibit promising capacity, further exploration was needed to validate the diagnostic ability of pharmacokinetic parameters, texture features and the mathematical regression analysis.

Acknowledgements

Not applicable.

Funding

No funding was received.

Availability of data and materials

The datasets analysis methods used during the current study are available from the corresponding author on reasonable request.

Authors' contributions

QLN was responsible for designing the study and drafting the manuscript. XMJ, QL, ZLZ performed the statistical analysis and researched the literature. HWD and SSW were responsible for the MRI scanning and XXZ contributed to DCE-MRI. All authors read and approved the final version of the manuscript.

Ethics approval and consent to participate

This study was approved by the institutional review board of The Wei Fang Traditional Chinese Hospital. Informed consent was obtained from all patients.

Consent for publication

Not applicable.

Competing interests

The authors declare that they have no competing interests.

References

1. Peters NH, Borel Rinkes IH, Zuithoff NP, Mali WP, Moons KG and Peeters PH: Meta-analysis of MR imaging in the diagnosis of breast lesions. Radiology 246: 116-124, 2008.
2. Yankeelov TE and Gore JC: Dynamic contrast enhanced magnetic resonance imaging in oncology: Theory, data acquisition, analysis, and examples. Curr Med Imaging Rev 3: 91-107, 2009.
3. Walkersamuel S, Leach MO and Collins DJ: Evaluation of response to treatment using DCE-MRI: The relationship between initial area under the gadolinium curve (IAUGC) and quantitative pharmacokinetic analysis. Phys Med Biol 51: 3593-3602, 2006.
4. Padhani AR, Gapinski CJ, Macvicar DA, Parker GJ, Suckling J, Revell PB, Leach MO, Dearnaley DP and Husband JE: Dynamic contrast enhanced MRI of prostate cancer: Correlation with morphology and tumour stage, histological grade and PSA. Clin Radiol 55: 99-109, 2000.
5. Yankeelov TE, Lepage M, Chakravarthy A, Broome EE, Niermann KJ, Kelley MC, Meszoely I, Mayer IA, Herman CR, McManus K, *et al*: Integration of quantitative DCE-MRI and ADC mapping to monitor treatment response in human breast cancer: Initial results. Magn Reson Imaging 25: 1-13, 2007.
6. Haralick RM, Shanmugam K and Dinstein I: Textural features for image classification. Syst Man Cybern IEEE Transact SMC-3: 610-621, 1973.
7. Holli K, Lääperi AL, Harrison L, Luukkaala T, Toivonen T, Ryymin P, Dastidar P, Soimakallio S and Eskola H: Characterization of breast cancer types by texture analysis of magnetic resonance images. Acad Radiol 17: 135-141, 2010.
8. Castellano G, Bonilha L, Li LM and Cendes F: Texture analysis of medical images. Clin Radiol 59: 1061-1069, 2004.
9. MacKay JW, Murray PJ, Kasmai B, Johnson G, Donell ST and Toms AP: MRI texture analysis of subchondral bone at the tibial plateau. Eur Radiol 26: 3034-3045, 2016.
10. Son JY, Lee HY, Lee KS, Kim JH, Han J, Jeong JY, Kwon OJ and Shim YM: Quantitative CT analysis of pulmonary ground-glass opacity nodules for the distinction of invasive adenocarcinoma from pre-invasive or minimally invasive adenocarcinoma. PLoS One 9: e104066, 2014.
11. Jain KK, Sahoo P, Tyagi R, Mehta A, Patir R, Vaishya S, Prakash N, Vasudev N and Gupta RK: Prospective glioma grading using single-dose dynamic contrast-enhanced perfusion MRI. Clin Radiol 70: 1128-1135, 2015.
12. Loose J, Harz TM, Laue H, Twellmann T, Bick U, Rominger M, Hahn HK and Peitgen HO: Assessment of texture analysis on DCE-MRI data for the differentiation of breast tumor lesions. Proceed SPIE-Int Soc Opt Eng 7260: 3113-3122, 2009.
13. Taoka T, Kawai H, Nakane T, Hori S, Ochi T, Miyasaka T, Sakamoto M, Kichikawa K and Naganawa S: Application of histogram analysis for the evaluation of vascular permeability in glioma by the K2 parameter obtained with the dynamic susceptibility contrast method: Comparisons with Ktrans obtained with the dynamic contrast enhance method and cerebral blood volume. Magn Reson Imaging 34: 896-901, 2016.
14. Chen X, Wei X, Yang R, Jiang X, Xu X and Jiang X: Differentiation of glioblastomas and solitary metastatic brain tumors using texture analysis of conventional MRI. Chin Med Abs, 2016. doi: 10.3760/cma.j.issn.1005-1201.2016.03.006.
15. Kido S, Katamoto A, Xu R and Hirano Y: Differential diagnosis of benign and malignant brain tumors by use of texture analysis on FDG-PET images. Radiol Soc North Am 2013 Sci Assem Meeting, 2013.
16. Tofts PS, Brix G, Buckley DL, Evelhoch JL, Henderson E, Knopp MV, Larsson HB, Lee TY, Mayr NA, Parker GJ, *et al*: Estimating kinetic parameters from dynamic contrast-enhanced t_1-weighted MRI of a diffusable tracer: Standardized quantities and symbols. J Magn Reson Imaging 10: 223-232, 1999.
17. Tofts PS: T_1-weighted DCE imaging concepts: Modelling, acquisition and analysis. Signal 500: 400, 2010.
18. Calamante F: Arterial input function in perfusion MRI: A comprehensive review. Prog Nucl Magn Reson Spectrosc 74: 1-32, 2013.
19. Bino SV, Unnikrishnan A and Balakrishnan K: Gray level co-occurrence matrices: Generalisation and some new features. Int J Com Sci Eng Informa 2: 151-157, 2012.
20. Leo HC, Evan LR and Richard DB: Fault diagnosis in chemical processes using Fisher discriminant analysis, discriminant partial least squares, and principal component analysis. Chemometr Intell Lab 50: 243-252, 2000.
21. Ostrovsky E, Zelig U, Gusakova I, Ariad S, Mordechai S, Nisky I and Kapilushnik J: Detection of cancer using advanced computerized analysis of infrared spectra of peripheral blood. IEEE Trans Biomed Eng 60: 343-353, 2013.
22. Dong L, Sun X, Chao Z, Zhang S, Zheng J, Gurung R, Du J, Shi J, Xu Y, Zhang Y and Wu J: Evaluation of FTIR spectroscopy as diagnostic tool for colorectal cancer using spectral analysis. Spectrochim Acta A Mol Biomol Spectrosc 122: 288-294, 2014.
23. Villeda VA, Benakanakere I and Freter C: The effect of cholesterol depletion in resistant breast cancer cells. J Clin Oncol, 2012.
24. Yim H, Kang DK, Jung YS, Jeon GS and Kim TH: Analysis of kinetic curve and model-based perfusion parameters on dynamic contrast enhanced MRI in breast cancer patients: Correlations with dominant stroma type. Magn Reson Imaging 34: 60-65, 2016.
25. Ryu JK, Sun JR, Song JY, Cho SH and Jahng GH: Characteristics of quantitative perfusion parameters on dynamic contrast-enhanced MRI in mammographically occult breast cancer. J Appl Clin Med Phys 17: 377-390, 2016.
26. Eyal E, Badikhi D, Furman-Haran E, Kelcz F, Kirshenbaum KJ and Degani H: Principal component analysis of breast DCE-MRI adjusted with a model-based method. J Magn Reson Imaging 30: 989-998, 2009.

27. Zheng X, Xiao L, Fan X, Huang N, Su Z and Xu X: Free breathing DCE-MRI with motion correction and its values for benign and malignant liver tumor differentiation. Radiol Infect Dis 2: 65-71, 2015.
28. Yu X, Lin M, Ye F, Ouyang H, Chen Y, Zhou C and Su Z: Comparison of contrast-enhanced isotropic 3D-GRE-T1WI sequence versus conventional non-isotropic sequence on preoperative staging of cervical cancer. PLoS One 10: e0122053, 2015.
29. Li X, Zhu Y, Kang H, Zhang Y, Liang H, Wang S and Zhang W: Glioma grading by microvascular permeability parameters derived from dynamic contrast-enhanced MRI and intratumoral susceptibility signal on susceptibility weighted imaging. Cancer Imaging 15: 4, 2015.
30. Méndez CA, Pizzorni Ferrarese F, Summers P, Petralia G and Menegaz G: DCE-MRI and DWI integration for breast lesions assessment and heterogeneity quantification. Int J Biomed Imaging 2012: 676808, 2012.
31. Coroller TP, Grossmann P, Hou Y, Rios Velazquez E, Leijenaar RT, Hermann G, Lambin P, Haibe-Kains B, Mak RH and Aerts HJ: CT-based radiomic signature predicts distant metastasis in lung adenocarcinoma. Radiother Oncol 114: 345-350, 2015.
32. Kickingereder P, Burth S, Wick A, Götz M, Eidel O, Schlemmer HP, Maier-Hein KH, Wick W, Bendszus M, Radbruch A and Bonekamp D: Radiomic profiling of glioblastoma: Identifying an imaging predictor of patient survival with improved performance over established clinical and radiologic risk models. Radiology 280: 880-889, 2016.
33. Eyal E, Badikhi D, Furman-Haran E, Kelcz F, Kirshenbaum KJ and Degani H: Principal component analysis of breast DCE-MRI adjusted with a model-based method. J Magn Reson Imaging 30: 989-998, 2009.
34. Raman SP, Schroeder JL, Huang P, Chen Y, Coquia SF, Kawamoto S and Fishman EK: Preliminary data using computed tomography texture analysis for the classification of hypervascular liver lesions: Generation of a predictive model on the basis of quantitative spatial frequency measurements-a work in progress. J Comput Assist Tomogr 39: 383-395, 2015.
35. Huang YQ, Liang CH, He L, Tian J, Liang CS, Chen X, Ma ZL and Liu ZY: Development and validation of a radiomics nomogram for preoperative prediction of lymph node metastasis in colorectal cancer. J Clin Oncol 34: 2157-2164, 2016.